IJMP

Application of Electrical Impedance Spectroscopy in Bladder Cancer Screening

Ahmad Keshtkar

Abstract

Introduction
Bladder cancer is the most common malignancy in elderly people and most bladder cancers are transitional cell carcinomas (TCC). Bladder pathology is usually investigated visually by cystoscopy and this technique can represent different conditions ranging from simple inflammation to flat CIS. However, biopsies must be taken from the suspected area to obtain diagnostic information. This is a relatively high cost procedure in terms of both time and money and is associated with discomfort for the patient and increased morbidity.

Materials and Methods
Electrical impedance spectroscopy (EIS), a minimally invasive screening technique, can be used to separate malignant areas from non-malignant areas in the urinary bladder. The feasibility of adapting this technique to screen bladder cancer, and abnormalities during cystoscopy has been explored and compared with histopathological evaluation of urinary bladder lesions. Both ex vivo and in vivo studies were carried out in this study.

Results
The impedance data were evaluated in both malignant and benign groups and a significant difference between these two groups was revealed. In all measurements, the impedivity of malignant bladder tissue was significantly higher than the benign tissue, especially at lower frequencies (p<0.001)

Conclusion
This technique can be a complimentary method for cystoscopy, biopsy, and histopathological evaluation of the bladder abnormalities.

Keywords: Bladder Cancer; Electrical Impedance Spectroscopy; Finite Element Modelling; Minimally Invasive Technique; ROC Curves

1- Medical Physics Department, Medical Faculty, Tabriz University of Medical Sciences, Tabriz, Iran
*Corresponding author: Tel & Fax: +98411 3364660; Email: mpp98ak@hotmail.com

1. Introduction

1.1. Clinical Background and application of EIS

Most of the bladder cancers are transitional cell carcinomas (TCC) and it is one of the commonest cancers, with approximately 13,000 new cases and 5,400 deaths per year in the UK [1]. This study investigates whether it is possible to diagnostically classify bladder mucosa using the minimally invasive technique of electrical impedance spectroscopy (EIS), which was developed initially to screen cervical cancer [2], and has subsequently been used in the assessment of Barrett's oesophagus [3]. The morphology of urothelium, and the natural history of pre-cancerous changes in urothelium, is significantly different from the changes in the cervix and oesophagus. The impedance spectrum generated by EIS is a function of the detailed structure of the tissue at the cellular level. Normal human urothelial mucosa consists of an epithelial layer 3–6 cells thick, a lamina propria of loose connective tissue, and a variable and discontinuous band of sub-mucosal muscle. In CIS, the umbrella cells usually disappear and are replaced by undifferentiated cells. Urothelial carcinoma *in situ* is characterized by flat, and disordered proliferation of urothelial cells with marked cytological abnormalities including nucleomegaly (increased nuclear size), nucleolomegaly (increased nucleoli size), pleomorphism (abnormally shaped cells), loss of cellular polarity, and mitoses. In inflammatory conditions, the white cells, small vessels, and fibrous tissue components of the lamina propria may all increase, sometimes dramatically. EIS measurements have been made on both fresh excised human bladders and, following development of a suitably small probe that could be passed down the biopsy channel of a cystoscope, *in vivo* during cystoscopy. The effect of fluid volume in the bladder and pressure on the probe tip, both of which would be expected to alter the impedance spectrum as a result of morphological changes, have been explored. Finite element modelling of the current flow at a cellular and macroscopic level in a simple model of the urothelium has been used to explore the spectral characteristics that are peculiar to urothelium. The feasibility of adapting bioimpedance technique to screen for bladder cancer and abnormalities during cystoscopy has been explored and compared with histopathological evaluation of urinary bladder lesions [4]. Ex vivo studies were carried out in this study by using a total of 30 measured points from malignant and 100 measured points from non-malignant areas of patients bladders in terms of their biopsy reports matching to the electrical impedance measurements. In all measurements, the impedivity of malignant area of bladder tissue was significantly higher than the impedivity of non-malignant area this tissue (P < 0.005). Finally, a study carried out to assess urinary bladder volume in a noninvasive manner using a portable and modified device that measures electrical impedance [5].

1.2. A review of existing bladder cancer detection techniques

There are different tests, but firstly because of simplicity, the patient will usually be asked for a urine sample, to test for blood and the possibility of urinary system infections. Various investigations are currently available to help with the diagnosis of bladder cancer as follows:

1.   **Diagnostic Radiology:** Conventional *X-ray* has long been used as a method to evaluate urinary system disorders.
2.   **Excretory Urography:** It is a type of *X-ray* examination specifically designed to study the kidneys, bladder, and ureters.
3.   **Urine Cytology:** Urine cytology is examining the urine samples of suspected patients under a microscope to look for cancerous or pre-cancerous cells. Urine cytology is often used to detect tumours because it is a simple and non-invasive technique.
4.   **CT scan and MRI:** Computed Tomography (CT scan) and Magnetic Resonance Imaging (MRI) use a narrow *X-ray* beam and radio waves respectively to take

detailed cross-sectional images of the organs. A computer then combines these images into a very detailed cross-sectional image. These images provide information about whether the cancer may have spread to tissue next to the bladder. These are used to assess large bulky tumours, lymphatic involvement, and the response of tumours to radiation or chemotherapy [6].

5.   Ultrasound Scans: These produce echoes of the urinary bladder tissues by using ultrasound waves and the pattern of echoes reflected by tissues can be useful in determining the size of a bladder tumour. This technique similar to CT Scan is unable to show accurately the depth of muscle invasion due to its inability to distinguish between individual layers of muscle wall [7].

6.   Cystoscopy: Visual examination of the urinary tract is possible with a cystoscope (a thin , and slender tube with a tiny camera attached and a light usually from a fibre optic cable). In this procedure, a cystoscope is placed into the bladder through the urethra and permits the doctor to inspect the inside of the urinary bladder if suspicious areas of growth are seen, and then a biopsy (removing a small piece of tissue) will be taken for further histopathological examinations. When we are using the cystoscope to see inside the bladder, CIS can be seen as a flat lesion (it can be difficult to diagnose) and cannot be differentiated from other erythematous potentially benign areas, because it may be a red patch or velvety in appearance but not always visible. Thus, a random biopsy and cytological analysis of the urine are required for definitive diagnosis. At present, definitive diagnosis can be made with a biopsy, usually under general anaesthesia, with resulting patient discomfort, increased morbidity, and relatively high cost. If the flexible type of cystoscope is used, it may not be painful and there is no need for a general anaesthetic procedure, but under some circumstances such as taking tissue samples (biopsies), general anaesthesia may be recommended. Therefore, cystoscopy and biopsy remain the gold standard and common urological procedures for bladder abnormalities.

In the light of this background, it is possible that electrical impedance spectroscopy may be appropriate for the early detection of flat lesions and assessing bladder pathology. This technique will be detailed in the following section. Thus, this study considers the introduction of a novel minimally invasive diagnostic technique to detect bladder cancer and other abnormalities of the human urinary bladder. This is because of the potential of the technique to separate pathologic epithelium from normal epithelium as a result of changes in cell size, cell arrangement, and extra-cellular space.

1.3. The aim of this study

The primary aim of this study is to develop a non-invasive screening technique to distinguish malignant and non-malignant areas in the urinary bladder. To achieve the primary aim, the secondary aims are to:

-Use computational modelling at a cellular level to investigate the effect of morphological changes on the impedance spectrum and inform the measurement regime.- Develop a probe which can be passed through the biopsy channel of a standard cystoscope to enable measurements to be taken *in vivo*. -Develop and validate techniques for comparing EIS measurements and histological sections in *ex vivo* bladders. -Develop and validate techniques for comparing EIS measurements and biopsies *in vivo*.-Determine the effect of bladder distension on the electrical impedance spectrum.

-Determine the effect on the electrical impedance spectrum of varying the pressure on the probe tip.- Compare impedance spectra, measured in *ex vivo* bladders, for tissue varying from normal to frank malignancy.-Compare impedance spectra, measured *in vivo*, for tissue varying from normal to frank malignancy.

Electrical impedance spectroscopy technique involves driving electrical currents through electrodes into the body, measuring the resulting potentials by the other electrodes,

and then calculating the transfer impedance. There are several researches working in this field such as a study which concerns the relationship between tissue structures and imposed electrical flow in cervical neoplasia carried out by Brown et al. to compare the impedance of normal and abnormal cervical tissues [2]. Another study investigated virtual biopsies in Barrett's oesophagus using electrical impedance measurements [3]. The aim of their study was to show the possibility of differentiating two types of epithelia (squamous and columnar) in terms of their electrical impedances. They have considered the inflammation effects on Barrett's oesophagus using low frequency system [8]. In the urinary bladder, initially, an attempt was made to distinguish the malignant (CIS and tumour) and benign (inflamed and normal) areas in the human bladder epithelium using electrical impedance technique at seven different frequencies [9]. Then, the same technique showed significant differences (p<0.05 at seven frequencies between 9.6 and 614 kHz) between normal and malignant urothelium (*ex vivo*), but was unable to classify individual measurements [10,11]. The same researchers used finite element technique to construct models of the urothelium and the underlying superficial lamina propria in order to ascertain the influence of structural changes associated with malignancy, oedema, and inflammation on the measured electrical properties of the tissue [12]. Therefore, it has been suggested that electrical impedance spectroscopy might be able to detect the urinary bladder malignancy.

2. Materials and Methods

The electrical impedance of the human urinary bladder was measured in 16 *ex vivo* bladder samples of 38 patients (*in vivo* study). These measurements were performed at 24 different frequencies in the frequency range of 2384 kHz using Mk3.5 Sheffield System, made by Sheffield University in UK. The applied current to measure the transfer impedance in this study was 10 μA peak-to-peaks. This

constant current passed through two electrodes of a small sized probe that was designed and constructed in the Medical Physics and Engineering Departments. However, Mk3.a Sheffield System (made by Sheffield University in UK) is working in seven different frequencies in the frequency range of 9.6614.4 kHz with 10 μA peak-to-peak current. There is a study which describes all properties of both systems carefully [13]. These electrodes were constructed of four gold wire electrodes, 0.5 mm in diameter, and spaced equally on a 1.6 mm diameter circle. Total diameter of the probe was only 2 mm thus it was limited because of the maximum permitted diameter of endoscopic channel to pass the probe towards the inside of the urinary bladder during the bladder surgery. Detailed information about this probe can be found in Keshtkar et al.[9] and Smallwood et al. [11]. As we know, the most common form of measuring tissue impedance is the tetra-polar or the four-electrode technique. This technique can measure transfer impedance (the ratio of measured voltage to applied current) of the urinary bladder. In this technique, a known current is driven between two electrodes and the resulting voltage is measured between the other two electrodes. Afterward, the resulting potential was measured using this technique to obtain the transfer impedance of the urothelium. This was used because it is designed to minimize the effect of electrode impedance on the measured data.

2.1. Probe design and construction

There are different steps in constructing this probe, which will be discussed. Initially, four sub-miniature coaxial cables, which are flexible, were fitted inside a medical grade Polytetraflouroethylene (PTFE) tube. This tube was used for in vivo bladder study because it can hold cables and electrodes closer and has a good compatibility with biological media. Moreover, the PTFE tube is flexible and has the ability to be wiped clean and allows the probe to be passed through the biopsy channel of a cystoscope into the urinary

bladder. In terms of tip designing process, the circular shape of the tip, instead of the planar shape, made the smallest configuration for our probe and thus this shape was chosen [14]. Then, different probe treatment processes were used to fix the tip inside the PTFE tube and seal the junction area of the tip and this tube to reduce mechanical shock and liquid leakage from the bladder into the probe similar to thevacuum plasma method, Liquid leakage test, and electrical connection test.

2.2. Probe calibration process

In impedance data collection procedure, the probe was regularly calibrated using known conductivity of saline solutions before any measurement procedure to have the tissue impedance readings in terms of the impedivity in $\Omega.m$. The measured impedance data was recorded using a computer for further analysis. The constructed probes were calibrated in a uniform isotropic medium (saline solution), which enables the transfer impedance measurements to be converted to the equivalent impedivity of a uniform isotropic medium in $\Omega.m$. Therefore, this value is independent of electrode configuration and probe dimensions and thus unifies the results. This means that if we measure one place on the tissue with each of the probes, the resulting impedances should be the same. Therefore, to ensure comparability between these probes, and before any electrical impedance measurement, the probe must be calibrated using different known conductivity saline solutions [14]. After analysing the impedance data using MATLAB software, the scatter and Cole equation fitting plots were prepared for both malignant and benign points of the bladder tissue. Moreover, before any impedance measurement (*in vivo*), the probe was sterilized for about one hour in the urology outpatient department.

2.3. Impedance measuring technique

For following the *in vivo* impedance measurement method, surgeon inspected whole of the urinary bladder using a flexible cystoscope. In this procedure, the cystoscope was inserted inside the bladder and a number of points were identified. These were marked using indigo carmine, a blue coloured liquid, via a 1 mm diameter sclerosing endoscopy needle. Therefore, the dye method was used to mark the measured point of the bladder. In addition, the measurement point was about 5 mm away from the colour marked point, thus the authors tried to cancel any possible side effects of the injected colour liquid on the measured real impedance of the bladder tissue. After colour marking the bladder, the cystoscope (including the probe) was inserted inside the bladder immediately and then it was used for finding the marked points to perform impedance measurements. Finally, the impedance readings were taken from near the marked point (about 5 mm away) using the probe inside the cystoscope. After obtaining each impedance reading, punch biopsies were taken from the measurement area and then they were fixed separately in formalin solution for standard histopathological examination (to compare the measured data with the pathological results). Histopathological assessment used in the first 500 μm depth of the sample, from the mucosal surface to represent the depth of the electrical impedance measurements. However, there was a sensitivity of about 95% for the electrical impedance measurements at this depth [15]. After different histopathological processes, the tissue samples were cut at 4 μm thickness using a microtome. Then, the sections were floated on water and were transferred to slides. Three sections were placed on each slide. Haemotoxylin and eosin staining was performed on all formalin-fixed, and paraffin embedded sections to see the epithelium and tissue morphology. The tissue sample was processed and viewed by a urology histopathologist under a light microscope to determine the organisation and shape of the cells. According to the reports, changes of the urothelium were classified histologically into benign, malignant, CIS, and inflammation groups with different degrees (0 = no inflammation, 1 = mild inflammation, 2 = moderate inflammation, and 3 = severe

inflammation). Every patient who participated in this study was asked to fill and sign a questionnaire (for *in vivo* measurements). It must be mentioned that in order to analyse data, a simple tissue equivalent model, the Cole equation model, was used. This model considers the tissue as a combination of two resistors and a capacitance: One resistor (R), the extra-cellular space which is in parallel with a series of a membrane capacitance (C) and another resistor (S), and the intra-cellular space. Therefore,"a non-linear least squares fitting programme" was used to fit this model to the measured impedance data [16]. Furthermore, to evaluate the significance of separating measured impedance spectrum, a non-parametric statistical test, the two-sample Kolmogorov-Smirnov test, was applied to these data. Finally, the Receiver Operating Characteristic (ROC) curves for the parameters R and $\dfrac{R}{S}$ was applied to evaluate the possibility of individual classifications of the benign and malignant points [10].

2.4. The effect of applied pressure on the electrical impedance of the bladder tissue using small and large probes

Different pressures were applied with this probe and both effect of the increasing pressure on the measured impedance of the bladder tissue and the effect of large size of the probe on the measured impedance data were studied (all of the measurements were taken on points that had benign histology). An excessive amount of applied pressure beyond the first visible indentation (first recordable reading) pressure was evaluated to find the effect on the impedance of the bladder tissue. Then, to assess the effect of pressure on the measured bioimpedance, the effect of the large size of the probe (10 mm diameter) was considered [17].

2.5. The effect of bladder volume changes on the measured electrical impedance of the bladder tissue

Furthermore, the bladder volume changes using some liquids to make the bladder distension, which were expected to affect the resulting electrical impedance of the urinary bladder (*in vivo* and *ex vivo*), were studied. Different volumes of bladders were assessed to measure their impedance using different solutions such as glycine. Then, the glycine solution volume was changed and repeated readings were made for different volumes of solution. This process was carried out for all of the patients. There were five patients' bladders assessed in this experiment to evaluate the effect of bladder distension on the resulting impedance of the urothelium. All of the patients were under anaesthesia. First of all, each measured point of the bladder was marked using indigo carmine to take the impedance reading about 2 mm away from this point. After that, each bladder was filled with a defined volume of glycine solution and an electrical impedance reading was immediately recorded from that point. The maximum volume for each bladder, the volume at which all of the mucosal folds are flattened, varied from patient to patient. Thus, different volumes of bladders were assessed to measure their impedance. Then, the glycine solution volume was changed and the readings were recorded repeatedly for different volumes. This process was carried out for all of the patients' bladders [18]

2.6. Modelled current distribution inside the normal and malignant human urothelium using finite element analysis

The current distribution inside the living tissue (the bladder tissue in this study) in every frequency was obtained using \the finite element technique [19]. When the tissue is changing from normal to abnormal, the distribution of tissue liquids between intra and extra cellular space will be changed and the measured conductivity and impedivity will also change. Therefore, it causes a different current distribution inside the human bladder tissue in normal and malignant cases. By knowing the amount of electrical impedance inside the bladder tissue and the morphological parameters of the different layers of this tissue, the current distribution inside the bladder tissue (surface

fluid, superficial urothelium, intermediate urothelium, basal urothelium, basement membrane, and connective tissue) was modelled and calculated in different frequencies using the finite element analysis [19].

3. Results and Discussion

3.1. Impedance measuring results

The relationship between the tissue impedance and frequency for malignant and benign areas are shown in Figure 1 [10]. The circular and rectangular points show the mean value of the real part of impedivity for every point in different frequencies (in $\Omega.m$). These are related to non-malignant and malignant areas, respectively. Box plot can demonstrate the impedance data distribution resulting from malignant and non-malignant areas. Thus, according to these plots, both data distributions are not normal [20]. Therefore, a non-parametric statistical technique, the two-sample Kolmogorov-Smirnov test was used to evaluate the significant difference between the malignant and benign areas. According to the calculation of respective data for the measurements, resistivity of the malignant group was higher than that of the non-malignant group at all of the frequencies ($p<0.001$), but it is clear that the overlapping of the groups will preclude the classification of individual measurements as normal or malignant. This figure shows the significant difference in mean values but there is an overlap of individual measurements [10].

Moreover, there is a plot that resulted from the Cole equation fitting extracted from the measured impedance data for both *ex vivo* and *in vivo* studies. There were 25 malignant and 98 benign points for *ex vivo*, and 24 and 73 points for *in vivo* studies, respectively. These points demonstrated a group separation between two malignant and benign groups from each other (Figure 2)[20].
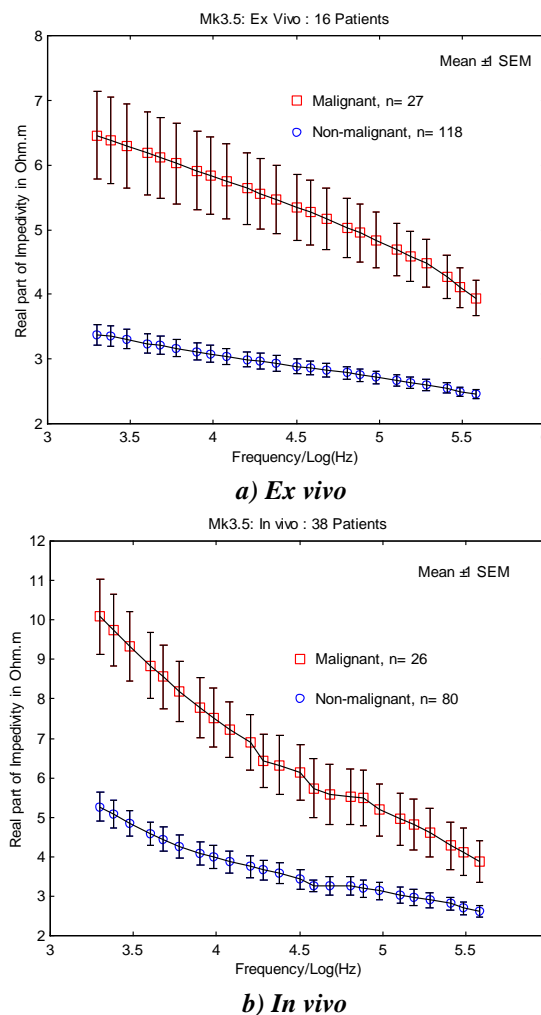

a) Ex vivo

b) In vivo

Figure 1. Real part of impedivity versus log of frequency for benign and malignant areas of the bladder tissue (*ex vivo* and *in vivo*). The error bars in this figure demonstrate standard error of mean

In fact, the Cole equation was fitted to the measured data. However, this model did not fit exactly to a number of measured points and thus the number of malignant and benign points is less than the real numbers. However, the number of malignant and benign points in Figure 2 is less than the number of the same points in Figure 1, respectively. The fitting software (MATLAB M.file) that author used in this study to fit the data was written by Waterworth. He introduced CNLSFIT software (Complex Non-linear Least Squares Fitting of the Cole equation to the measured or simulated data) [16].The parameters R, S, and C were used as fitting parameters. The real part of impedivity was used to separate

malignant points from the benign area of the urinary bladder. It means that due to the determination of extra-cellular and intra-cellular impedivities from the Cole equation model, the malignant and benign points are placed in right hand and left hand sides of this figure, respectively [10].

The scatter plot suggests that classification of malignant areas may be possible, but the false-negative and false -positive rates may be high. This has been explored using (ROC) curves for the parameters R and $\frac{R}{S}$ separately similar to the work done by [21]. These parameters are shown in Figures 3 and 4 and show that individual classification is possible. The areas under the curves are shown and the standard error for the area under the curve is calculated using the following equation:

$$SE = \sqrt{\frac{\theta(1-\theta) + (n_A - 1)(Q_1 - \theta^2) + (n_N - 1)(Q_2 - \theta^2)}{n_A n_N}}$$

here θ is the area under the curve, and n_A and n_N are the number of abnormal and normal, respectively. Q_1 and Q_2 are estimated using $Q_1 = \frac{\theta}{(2-\theta)}$ and $Q_2 = \frac{2\theta^2}{(1+\theta)}$.
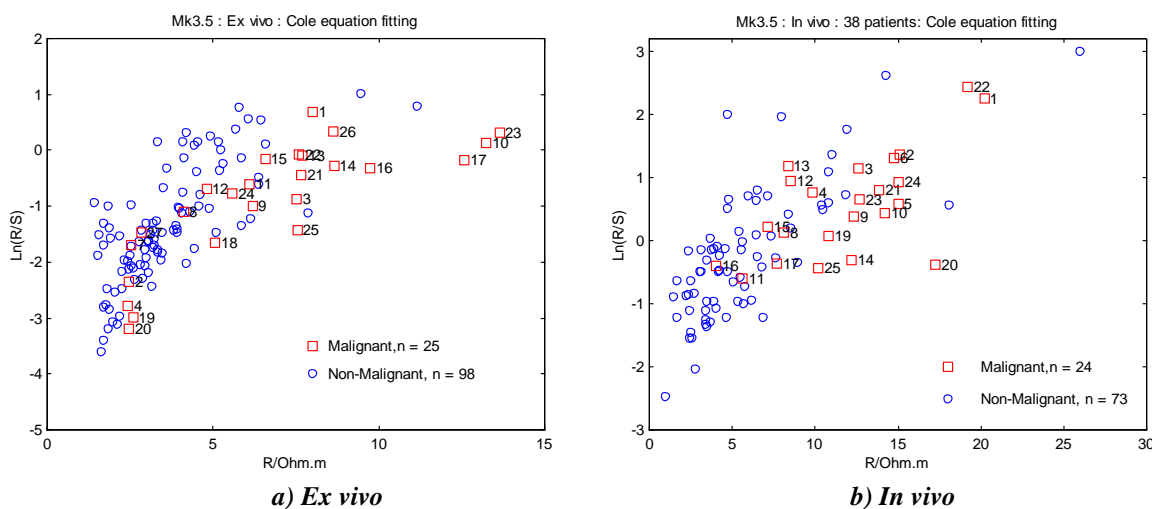
a) Ex vivo

b) In vivo

Figure 2. The Cole equation fitting for benign and malignant areas of the bladder tissue (*ex vivo* and *in vivo*) [10]

(a)

(b)
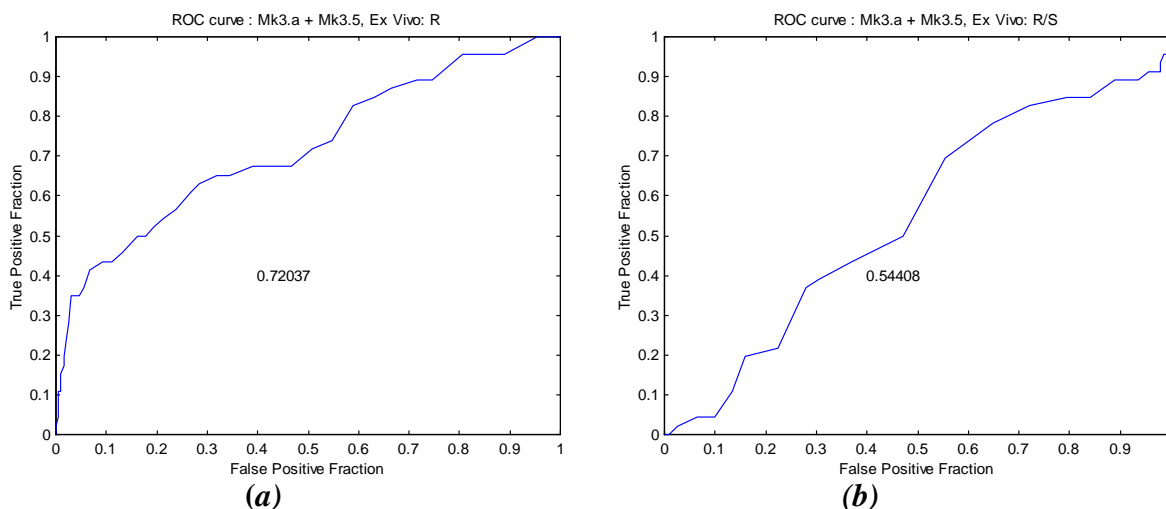
Figure 3. The ROC curve for the parameters R and $\frac{R}{S}$ (Ex *vivo* study): a) R b) $\frac{R}{S}$ [10]
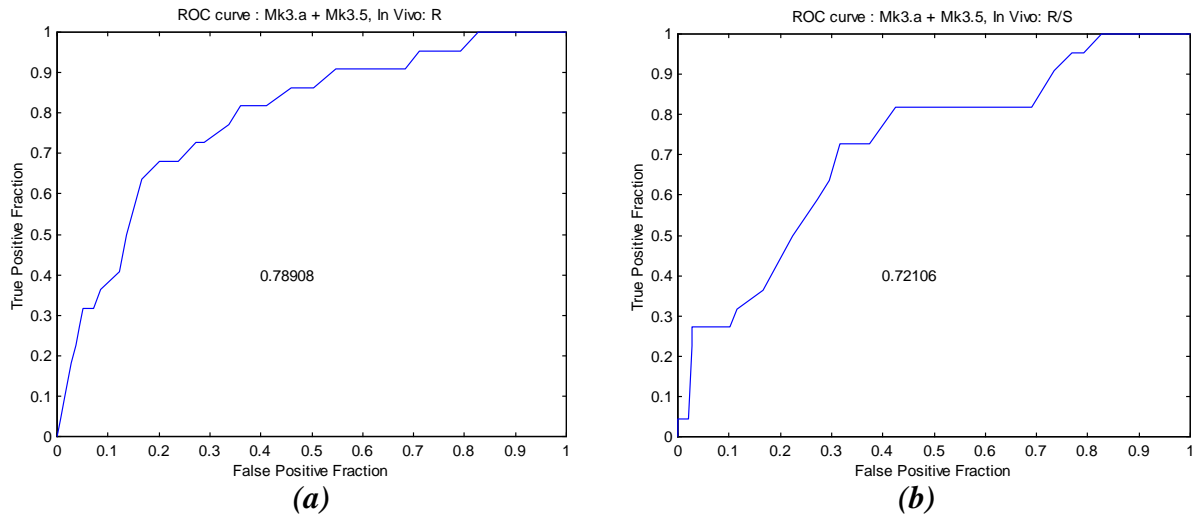
(a)   *(b)*

Figure 4. The ROC curve for the parameters R and $\dfrac{R}{S}$ (In *vivo* study): a) R b) $\dfrac{R}{S}$ [10]

a   *b*

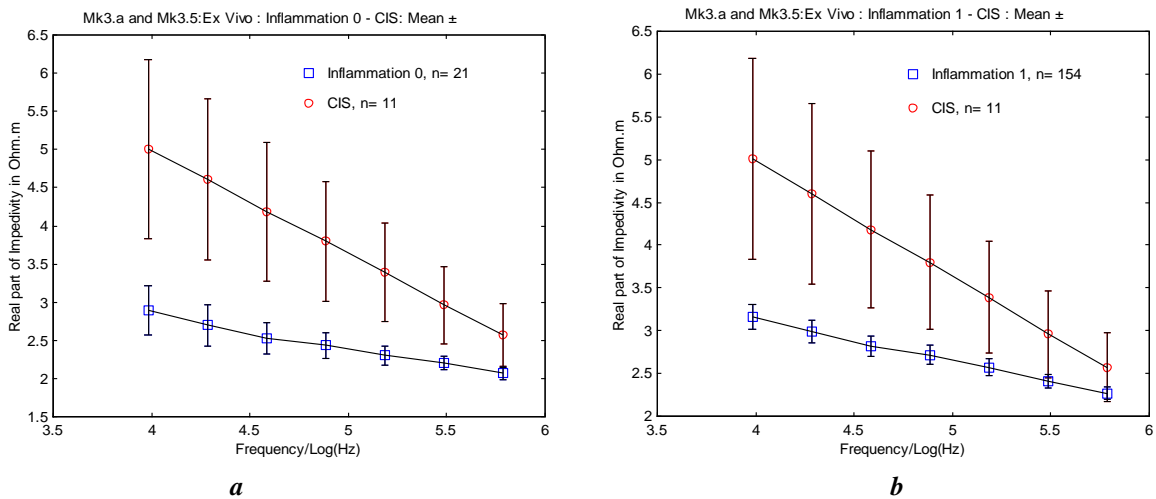Figure 5. Differentiating CIS from inflammation grades 0 (a) and 1 (b) of the bladder tissue in seven different frequencies (error bars are mean±1 standard error of mean), [10].
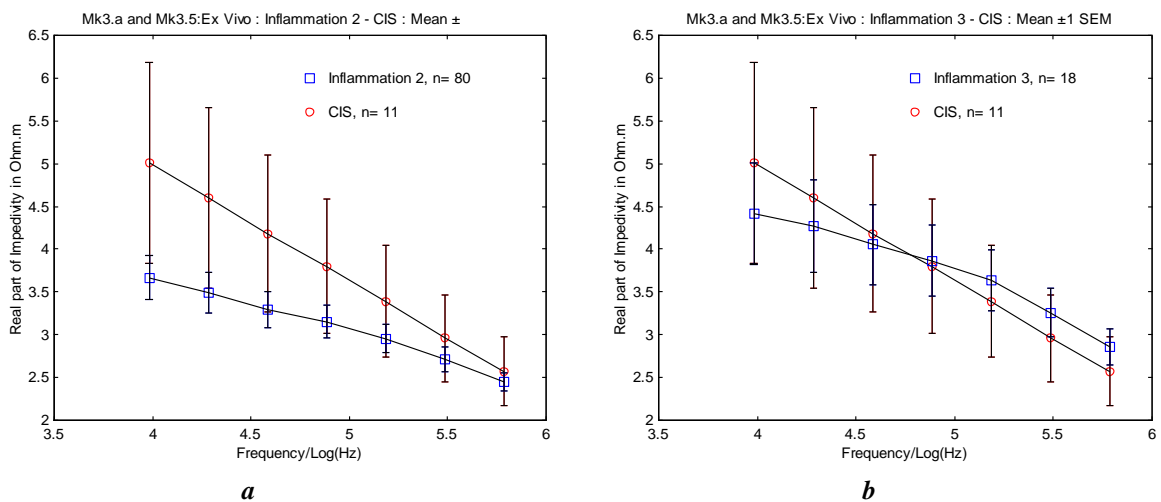

a   *b*

Figure 6. Differentiating CIS from inflammation grades 2 (a) and 3 (b) of the bladder tissue (error bars are mean ±1 standard error of mean) [10]
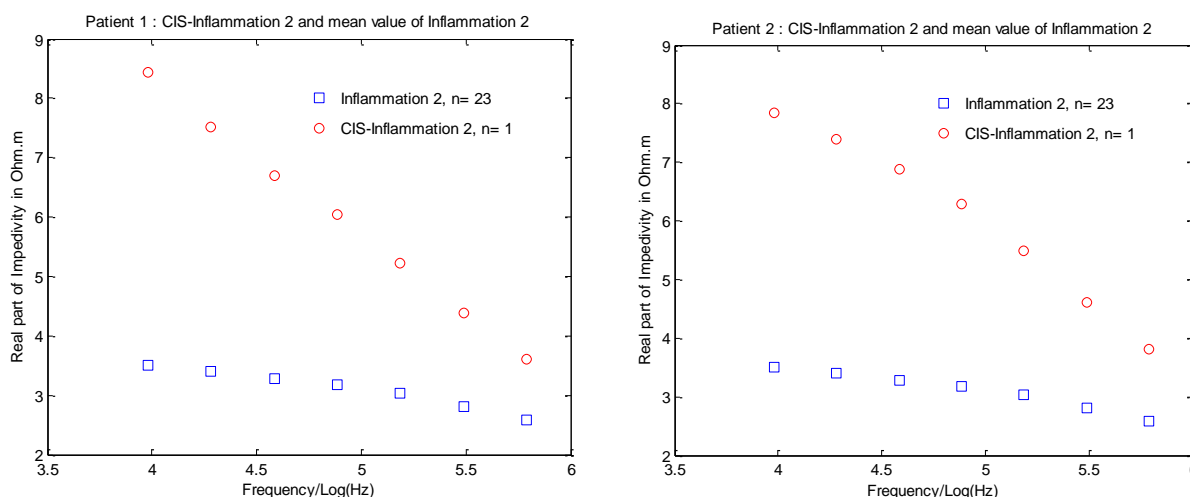
Figure 7. Differentiating CIS inflammation grade 2 from inflammation grade 2 (from two patients) [10]

Furthermore, separation of carcinoma *in situ* (CIS) from the inflammation area with different degrees of inflammation (no=0, mild=1, moderate=2, and severe inflammation=3) is presented in Figures 5 and 6.

Two plots in Figure 5 enable differentiation of the CIS measured data from the inflammation data (grades 0 and 1) ($p < 0.01$) (The number of measured data is 11 CIS, 21 Inflammation 0, and 154 Inflammation 1) [10]. However, Figures 6a and 6b show no significant difference between CIS measured data and inflammation data (grade 2 [$p < 0.3$] and grade 3 [$p < 0.4$]) (The number of measured data is 11 CIS, 80 Inflammation 2, and 18 Inflammation 3).

Finally, there is a significant difference between CIS inflammation grade 2 and inflammation grade 2 ($p < 0.001$) as shown in Figure 7 (The number of measured data is 1 CISinflammation grade 2 and 23 inflammation 2). It is clear that in CIS inflammation case, the measured samples are related to both CIS and inflammation groups.

3.2. The measured data due to increasing pressure

According to the Cole equation fitting programme, the resulted plot demonstrates the applied low (0.00-31.24 kPa) and high (31.24-624.80 kPa) pressure effects on the measured impedance using the small probe, 2 mm total

diameter (Figure 8). In this figure, the readings of the high pressure are usually distributed in right hand side and the results of the applied low pressure are in left hand side compared with each other. This Cole equation fitting programme was explained by Cole in 1941 [22] and it was modified by Waterworth in 2000 [16]. There is a detailed discussion about this fitting procedure [10].
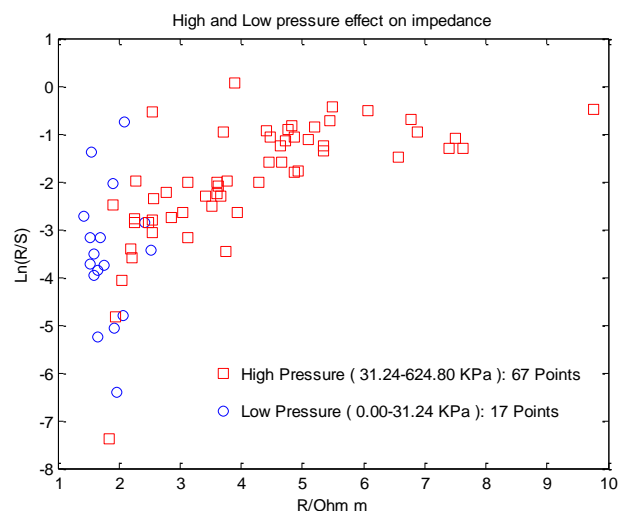

Figure 8. Effect of different applied pressures (Low: 0.00-31.24 kPa and High: 31.24-624.80 kPa) on the electrical impedance using small probe. R and S in the Cole equation fitting to the measured data are the extra-cellular and the intra-cellular impedivity, respectively (Ln is the natural logarithm of R/S)

3.3. Measured impedance resulted from different pressure groups

There is smaller variation in the resulted impedance using low pressures (Figure 9a) than applying high pressures (Figure 9b) on the same point of the bladder tissue. For example, there is a variation of 1.74-1.92 $\Omega.m$ for low and 4.78-5.39 $\Omega.m$ for high pressure in the frequency of 2 kHz. Because of these two different ranges of pressures and their related impedances, different ranges of impedivity are used to obtain these plots. Finally, it must be mentioned that there is no response from electrical impedance measurement system to the applied high pressures at higher frequencies (more than 153.600 kHz) in Figure 9b (the measurement system did not show anything in this range). Following the minimum applied pressure (having the first visible indentation on the bladder tissue), the effect of different applied pressures over the bladder tissue was considered (by increasing the applied pressures). For this purpose, the impedance measurements procedure was performed per point from seven different applied pressure groups (Table 1). The number of chosen measurements from these pressure groups is shown in the second column of the table. However, the number of measurements in different groups is varied because the ability of various parts of the bladder tissues to respond to the respected applied pressure is usually different [17].

Table 1. Seven pressure groups were used to assess the effect of applied pressure on the measured impedance in three resected bladders (kPa=Kilopascal)

Groups	Number of Measurements	Applied Pressure (kPa)
Group 1	8	0.00-15.65
Group 2	11	15.65-31.24
Group 3	16	31.24-62.60
Group 4	17	62.60-125.20
Group 5	16	125.20-219.10
Group 6	11	219.10-375.60
Group 7	8	375.60-626.80

After plotting the impedivity related to the different pressure groups against frequency, the effect of different pressure groups from the Table 1 on the measured impedance data is shown using the small probe (Figure 10).
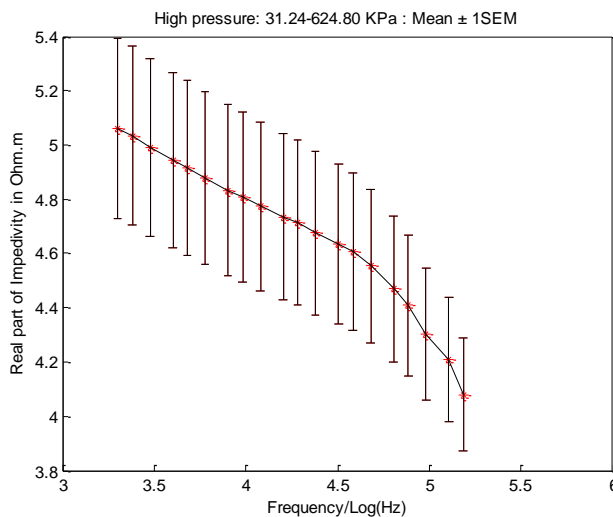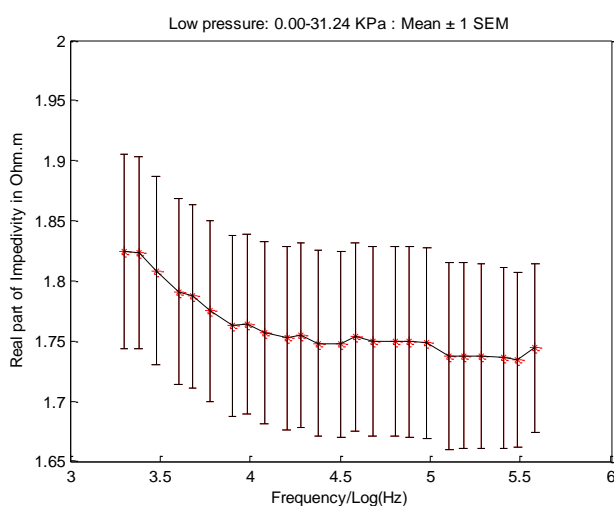

Figure 9. Effect of applied pressure on the measured electrical impedance of the bladder tissue using small probe (from 87 measurements): (a) Low pressure: 8+11=19 measurements, (b) High pressure: 68 measurements. For every case, an error bar plot is presented to show the mean value of the impedance on the low and high pressure group including 1 standard error of mean (SEM).
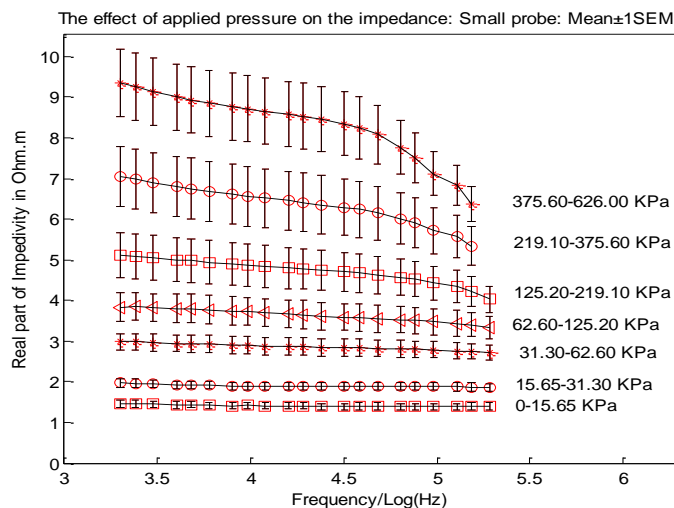
Figure 10. Effect of applied pressure on the electrical impedance using small probe. For every case, an error bar plot is presented to show the mean value of the impedance on seven pressure groups including 1 SEM [17].
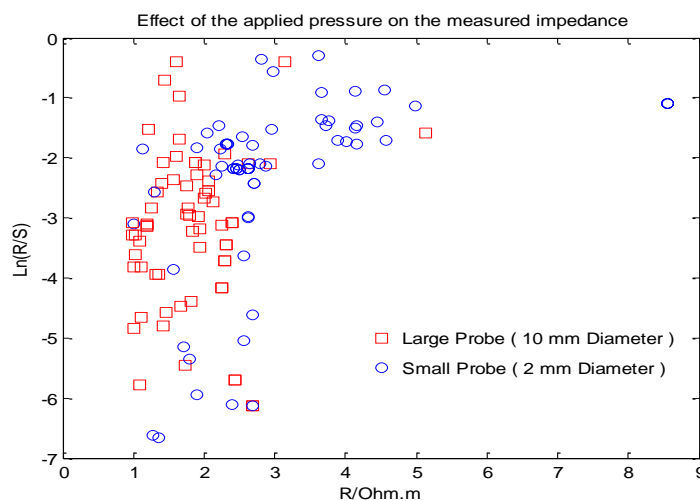
Figure 11. Effect of applied pressure (five pressure groups, from Table 2) on the electrical impedance using small and large probes over two resected bladders. R and S are the extra-cellular and the intra-cellular impedivity respectively [17].

Table 2. Pressure groups were used to assess the effect of probe contact area on the measured impedance using two resected bladders (kPa, mN=miliNewton).

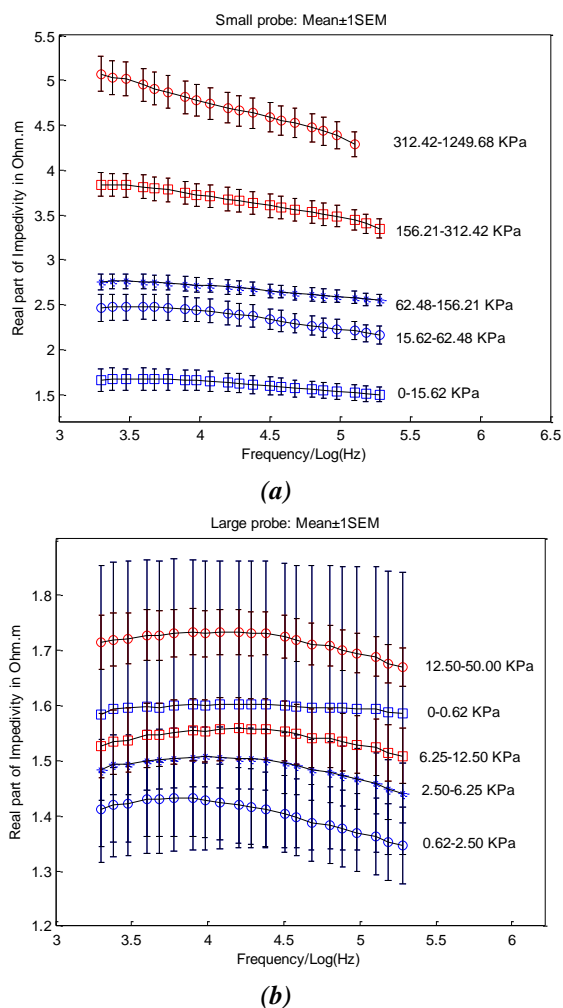| Groups	*Number of measurements / Applied pressure (kPa)*				Applied Force (mN)
	Small probe		Large probe		
Group 1	28	0.00-15.62	5	0.00-0.62	0.00-49.05
Group 2	24	15.62-62.48	40	0.62-2.50	49.05-196.20
Group 3	34	62.48-156.21	30	2.50-6.25	196.20-490.5
Group 4	45	156.21-312.42	38	6.25-12.50	490.5-981.0
Group 5	86	312.42-1249.68	112	12.50-50.00	981.0-3924.0

(a)

(b)

Figure 12. Effect of applied pressure (five pressure groups, from Table 2) on the electrical impedance using small and large probes over two resected bladders: (a) Small probe, (b) Large probe. For every case, an error bar plot is presented to show the mean value of the impedance on different pressure groups including 1 SEM [17].

3.4. The effect of probe sizes on the resulted impedance

There is another scatter plot resulted from the Cole equation fitting to the measured impedance data using small and large probes. In this figure, the readings of the small probe are usually distributed in right hand side and the results of the large probe are in the left hand side compared with each other (Figure 11).

Finally, the effect of applied pressure (five pressure groups, Table 2) on the electrical impedance using both small and large probes is demonstrated in Figure 12. In this figure, (a) and (b), the applied forces corresponding to the applied pressures (in every group) for both

probes are similar but their applied pressures were different because of their different diameters (Table 2). This experiment carried out over two resected bladders to compare the reproducibility of impedance measurements because of the probe sizes [17].

3.5. Surface fluids effects on the bladder tissue (Ex vivo study)

First of all, the impedivity of the surface fluids was measured three times and then averaged using the impedance measurement system. The volume of these fluids was about 100 ml at body temperature (Figure 13) [18]. This figure demonstrates that the impedance of glycine ($\cong 50 \Omega m$) is about 100 times larger than that of saline ($\cong 0.5 \Omega m$). Then, three human bladders were submerged in different surface fluids and the impedance of malignant (3 points of bladder 1 and 1 point of bladder 3) and benign (7 points of bladder 1, 10 points of bladder, 2 and 9 points of bladder 3) points were measured. Each measured point included 3 separated impedance readings because of reproducibility. Thus, the total number of measured malignant points was $4 \times 3 = 12$ and for non-malignant it was $26 \times 3 = 78$.

The volume of these liquids was about 100 ml. Note that the system failed to obtain several readings at certain frequencies because these points were out of the probe calibration range (the data represent the mean of 3 readings per point for reason of reproducibility). As Figure 14 shows, there are three plots of the bladder submerged in air (Figure 14a), saline solution (Figure 6b), and glycine solution (Figure 14c). The two-sample Kolmogorov-Smirnov test was used at each frequency because the data distribution was not normal. There was a significant difference between the impedance of malignant and non-malignant points using air ($p < 0.0001$), saline solution ($p < 0.001$), and glycine solution ($p < 0.001$) [18]. This statistical technique is similar to the work described in Keshtkar et al. in 2006 [10]. Therefore, these three plots show a significant differentiation of malignant and non-malignant groups from each other. These plots also show that the measured data for the bladder with

glycine has higher impedance than the bladder with air. Therefore, the electrical impedance of the bladder filled with air is more than the bladder filled with saline solution at all frequencies and in both malignant and non-malignant states.

Another plot compares the measured impedance data of malignant and non-malignant groups in the presence of previously mentioned materials (Figure 15). The reason for this study was to evaluate the effects of different fluids on the electrical impedances of both malignant and benign areas.
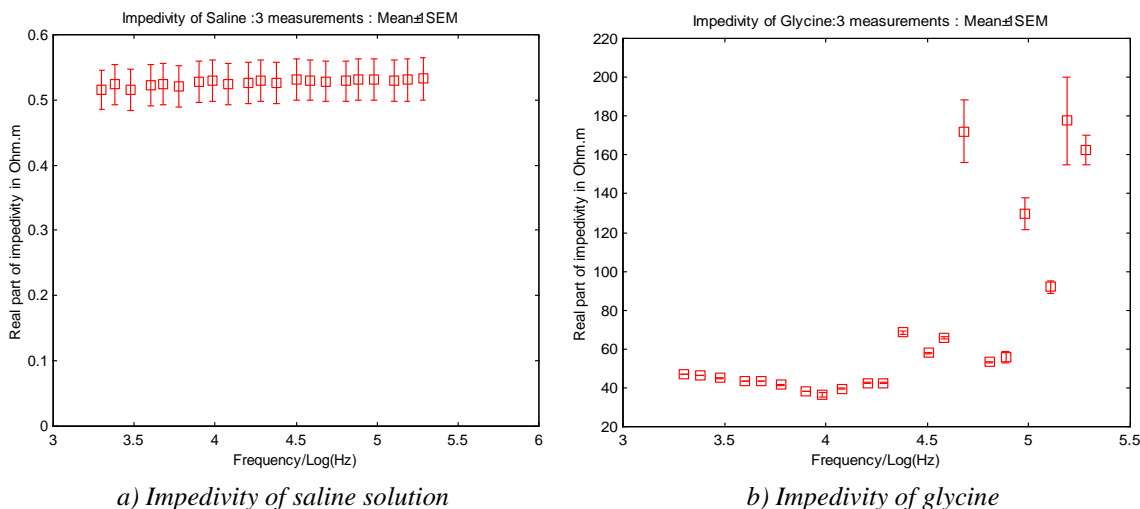

a) Impedivity of saline solution
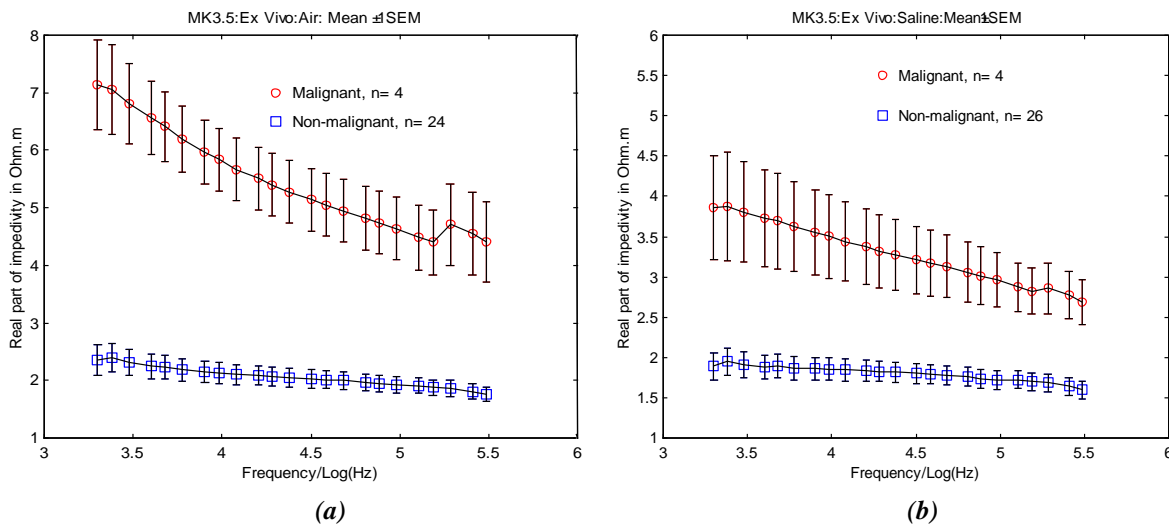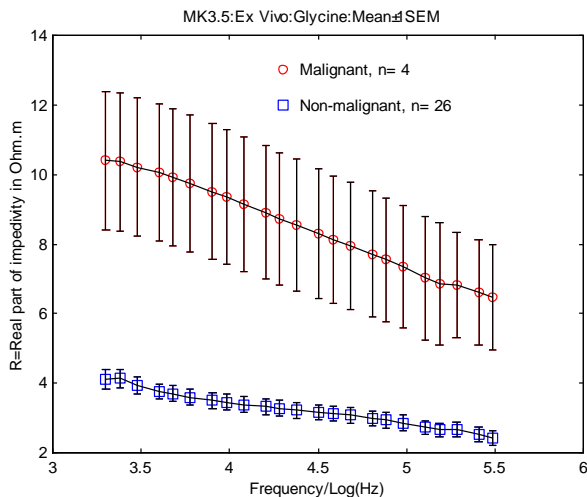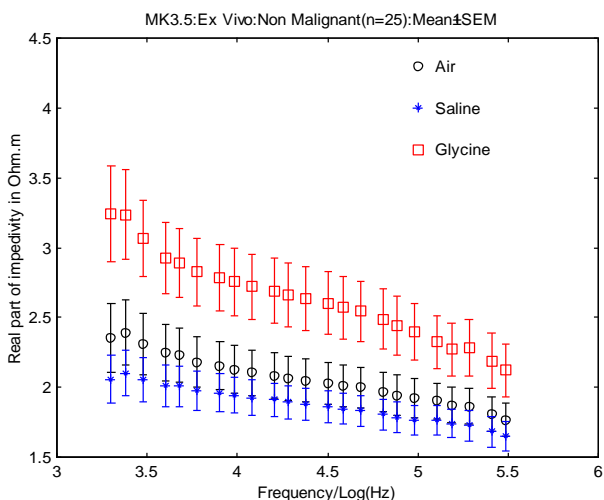
b) Impedivity of glycine

Figure 13. Impedivity of saline (a) and glycine (b) solutions at 21 frequencies (2-192 kHz).
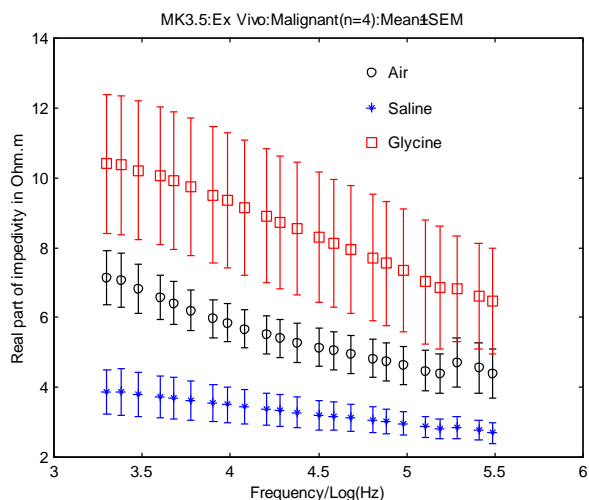

(a)

(b)

(c)

Figure 14. a) Comparison of Malignant (n=4) and non-malignant (n=26) points in air, b) Comparison of malignant (n=4) and non-malignant (n=26) points in saline solution (0.9%), c) Comparison of malignant (n=4) and non-malignant (n=26) points in glycine (1.5 %) [18]

(a)

(b)

Figure 15. Comparison of the impedance of a) Non-malignant points (n=25) and b) Malignant points (n=4) in air, saline (0.9 %), and glycine (1.5 %) (each point is the average of three separated readings because of reproducibility) [18]

It is clear from these figures that there is a difference in the electrical impedance for malignant and non-malignant points. However, in all cases, for glycine, the impedivity is more than air and for air it is more than saline. The two-sample Kolmogorov-Smirnov test was used at each frequency because the data distribution was not normal. There was no significant difference between measured data of non-malignant points using air-saline , and air-glycine but therewas a significant difference between saline-glycine (p<0.02) [18]. In addition, for malignant cases, there was no significant difference between air-saline , and

air-glycine but there was a significant difference between saline-glycine (p<0.001) [18]. If we use glycine or saline in our electrical impedance measurements, the measurement will be dominated by their high and low impedivity, respectively rather than the tissue impedivity. Thus, the possible reason that the results in Figure 15 (a) and 15 (b) are different for malignant and non-malignant groups may be due to fluids (running) between probe and tissue. It is clear that the type of surface fluid has a significant effect on the measured data. Generally, the impedance taken in glycine is of the order of 1.3-2 -fold greater than readings

taken in air (especially at lower frequencies) and in saline this ratio is 20% lower than in air [18].

3.6. Surface fluids effects on the bladder tissue (In vivo study)

As mentioned above, a total of six points (all benign) from three bladders were compared in resultant impedance using saline and glycine fluids separately (Figure 16). Each measured point included 3 separated impedance readings. This figure shows that the mean value of impedance when we used glycine was higher than when saline was used (approximately 3-fold increase). There is a significant difference in measured impedance between the six points of the bladder urothelium when the bladder included saline and then glycine (p<0.03). Although the measured impedance using glycine is significantly more than the impedance using saline solution (*in vivo*) and the mean value of impedance in saline cases seems to be the same as *ex vivo* results, the mean value of impedance for glycine cases for *in vivo* and *ex vivo* cases is different (compare Figure 15 (a) and Figure 16 for saline and glycine results). This difference may be due to the small number (6) of measurements (the lack of measurements) for *in vivo* study [18].
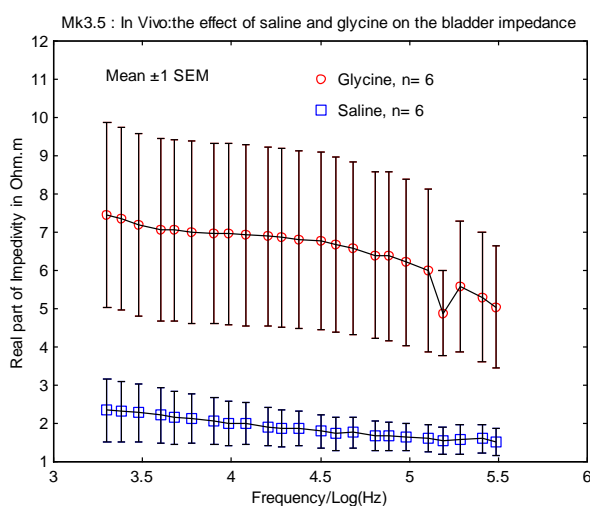

Figure 16.   Comparison of the Non-malignant bladder impedance when it is submerged in saline and then glycine (*in vivo*). [18]

3.7. Modelled current distribution inside the normal and malignant human urothelium using finite element analysis

Current was applied to the drive electrodes in the macroscopic model in the frequency range 100 Hz -10 MHz and voltages were calculated at the receiver electrodes in an identical arrangement to the tissue measurements. The current flowing through every node located on the boundary midway between the two drive electrodes could also be calculated and then integrated to give the total current flowing through each layer. This information can provide an indication of the current distribution, and hence the depth sensitivity of the probe. Various model parameters can be altered at either the cellular or the macroscopic stage of the modelling process in order to assess the effect on the impedance spectrum or the current distribution. Models were solved with mucus layer thicknesses in the range 5100 μm. The current distribution inside the bladder tissue using the computational modelling (finite element analysis) is shown in Figure 17 [18].

We can increase our knowledge to understand this behaviour by examining the current distribution in the normal and malignant models in the following sentences: Figure 18a shows the proportion of the total current flowing through each of the macroscopic model layers − surface fluid, superficial urothelium, intermediate urothelium, basal urothelium, basement membrane, and connective tissue, respectively, in the normal tissue model. Data are shown for a number of frequencies and for three thickness of surface fluid. Figure 18b shows similar data for the malignant tissue model. It is clear that very little of the current actually flows through the urothelium itself (layers 2-4), but is divided between the surface fluid and underlying connective tissue at a ratio which depends on current frequency, depth of surface fluid, and urothelial pathology [19].
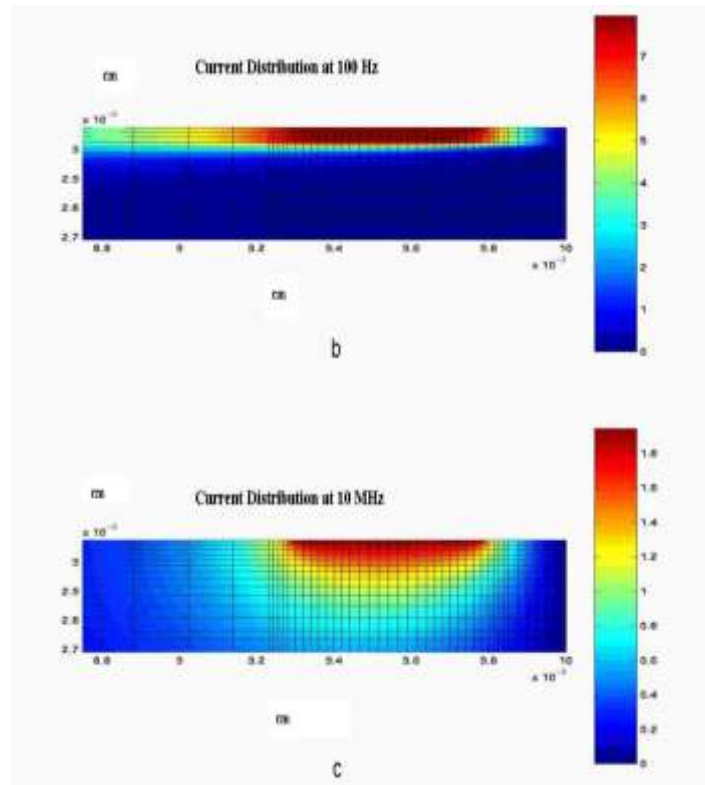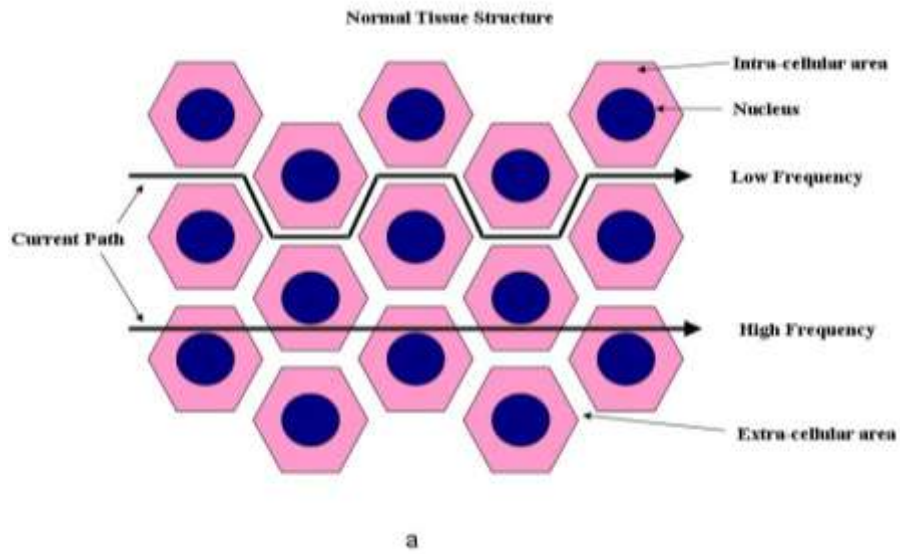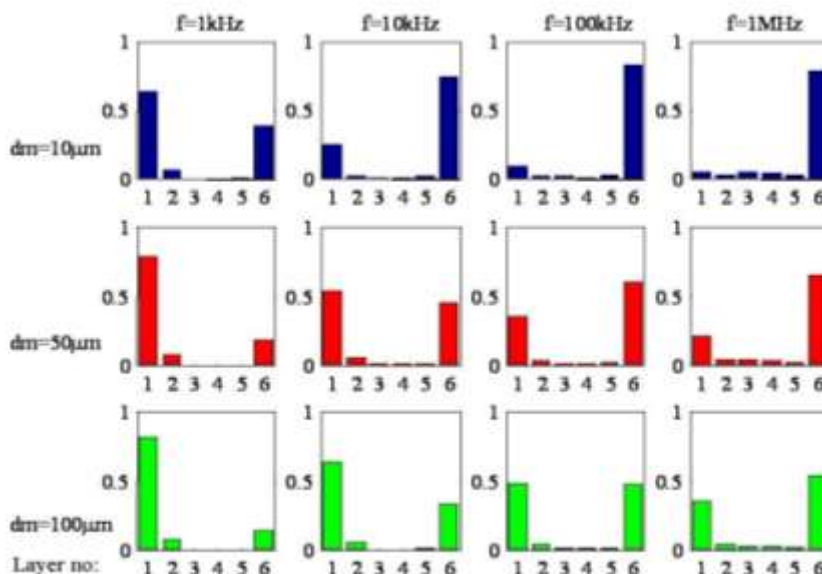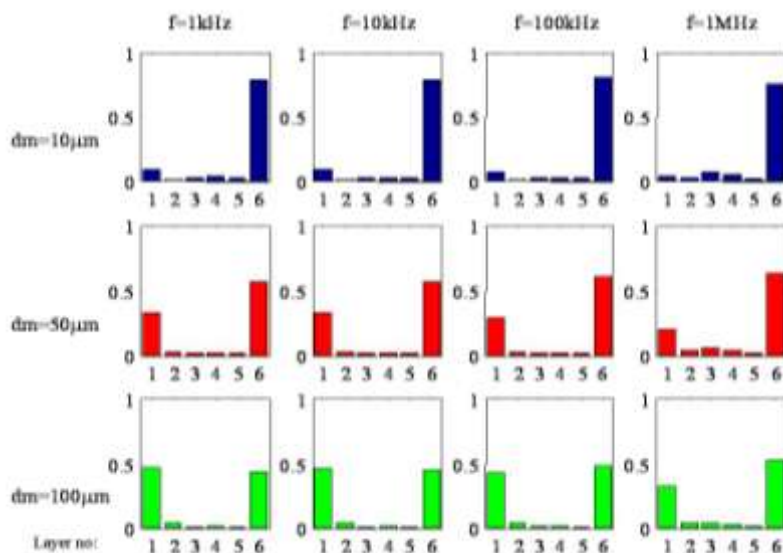
Figure 17. (a) Electrical current passes through the living tissue (in low and high frequencies). Computational modelling results for the current sensitivity distribution of the urinary bladder at low frequency, 100 Hz (b) and at high frequency, 10 MHz (c) [18]

(a)

(b)

Figure 18. Modelled current – depth distribution midway between drive electrodes for (a) Normal tissue model, (b) Malignant tissue model at different frequencies and surface layer thicknesses (dm) Layer no. key: 1 – surface fluid, 2-superficial urothelium, 3-intermediate urothelium, 4-basal urothelium, 5- basement membrane, and 6- connective tissue [18]

In the case of normal tissue, the presence of tight junctions and narrow intercellular spaces forms a very high impedance barrier, and at low frequencies in particular, current is confined to the surface fluid. As the frequency is increased, the capacitive nature of cell membranes allows current flow into the surface cells, effectively 'short-circuiting' the tight junctions and allowing current to penetrate beneath the epithelium and into the relatively high connective tissue beneath, thus causing the characteristic drop in

tissue impedance with increasing frequency. However, our malignant superficial cell models do not include tight junctions, and the extra-cellular space is also wider. Therefore, the barrier to current flow is greatly reduced, even at low frequencies. Figure 18b shows that at least 50% of the injected current flows beneath transformed urothelium across the frequency range modelled. However, in constructing the computational models of normal and malignant urothelium, due to the limited availability of

data, we had to make a number of assumptions about tissue structure and the electrical properties. For example, surface plaques were not included in this model, and though these structures were extremely small. The model results, Figure 18, show that much of the injected current flows through the connective tissue beneath the urothelium. Moreover, modelling of other squamous epithelia (e.g., cervix) has shown that the changes in the impedance spectrum associated with neoplasia were primarily due to the increase in the volume of the extra-cellular space (ECS). The fact that the measurements on bladder tissue yield the opposite results to those on cervix, i.e., an increase in low frequency impedance for malignant tissue compared to normal tissue suggest that there is a reduction in the volume of ECS associated with the malignancy of the bladder, or the structure of bladder tissue is significantly different to cervix in other respects, leading to a completely different distribution of current flow. In addition, bladder urothelium is also much thinner than cervical epithelium (approximately 80 μm compared with 300-400 μm), which suggests that current flow in the lamina propria may be even more important than the current flow in cervical stroma [19].

4. Conclusion

It is clear that an area of CIS is flat and these lesions cannot be differentiated from other benign flat areas using cystoscopy because they look macroscopically normal. This means that this area cannot be distinguished from other red patches or benign areas of the urothelium and thus the only diagnostic technique is random biopsies. However, if we use this technique in patients with the suspected disease, it is possible that no lesion will be found. Because of these difficulties, the search for other detection methods continues. This is the rationale for developing an alternative technique to scan the whole of the bladder and gain useful diagnostic information as soon as possible. Moreover, in this study, over the frequency range, the impedivity of the malignant area of the urothelium was significantly higher than that of the benign area especially at lower

frequencies. In fact, this is in contrast with the above-mentioned results. Extension of the measurements to lower frequencies showed an increasing separation of the impedance spectra at low frequencies. The electrical impedance data of the human urothelium were measured using Mk3.a and Mk3.5 Sheffield Systems and compared with histopathological reports of the biopsies, which were taken from the measurement area. These impedance data distributions were evaluated in both *ex vivo* and *in vivo* cases. However, the separation of these readings related to the malignant and non-malignant groups were evaluated in each case and revealed a significant difference between these two groups, especially at lower frequencies. The impedance of malignant and benign areas for the *in vivo* study were slightly higher than the impedance of these areas in the *ex vivo* study. Possible reason is the time between the bladder resection and taking impedance data for the *ex vivo* study. This can decrease the impedance of the bladder tissue in the *ex vivo* case relative to the time duration.

It is clearly seen from the results that the impedance measurements using small sized probe is not perfectly reproducible and therefore the effect of different applied pressures can be a major problem. Thus, this effect was assessed here to find a proper way to make a good reproducible reading of impedance changes due to the different applied pressures (the probe was completely in contact with the bladder tissue). Moreover, the impedance difference between the malignant and benign tissue is usually more than the difference caused by applying a little different pressures over the probe. Sometimes the impedance difference between benign and malignant tissue is not significant and as a result the applied pressure effect on the reading impedance will be very important and should be controlled carefully. It is clear from Figure 10 that there is a stepwise increase of the impedance at all of the frequencies from one pressure group to the next with a significant difference according to a non-parametric test, two-sample Kolmogorov-Smirnov test (p<0.001).

It was expected that the application of common surface fluids (air, saline solution, and glycine

solution) in the bladder epithelium would affect the measured electrical impedance of the urothelium. Therefore, the impedance measurements in this study showed clearly a difference in the impedance of the bladder tissue using surface fluids such as air, saline, and glycine solutions. In fact, the impedance was 1.3-2 -fold greater when we take the readings in glycine than in air. Moreover, this measurement for saline is about 20% lower than in the air. However, the measured impedance is usually variable between the impedance of saline ($0.5\Omega m$) and glycine ($50\Omega m$). This impedance is highest when we use glycine solution and lowest if the saline solution is used as the surface fluid. Anyway, the electrical impedance of the human bladder tissue for the malignant area is higher than for the benign area. Furthermore, the best fluid between air, glycine, and saline to measure the impedance of the urinary bladder is air ($p \langle 0.0001$) because of the greater separation of malignant and benign points when used inside the bladder. For consistency, it is essential to always use the glycine in the bladder during impedance measurements (*in vivo*). Furthermore, computational modelling is a good technique that allows us to improve our understanding of the current distribution inside tissue, and hence electrical impedance method as a potential diagnostic technique. Electrical impedance myography is a form of muscle assessment based on the surface application of electrical current and measurement of the resulting voltages over a muscle group of interest. In order to better understand the effect of pathological change in muscle, this has recently been applied to the rat. In this study, a finite element model is presented for the rat hind limb which incorporates the detailed anatomy of the leg based on computerized tomographic imaging and conductivity and permittivity values obtained from the rat gastrocnemius muscle. The model successfully predicts the recorded surface impedances measured with electrical impedance myography [23]. Therefore, finite element models of the bladder tissue were constructed in both cellular and macroscopic tissue levels. The model results show that very little of the current actually flows through the urothelium and much of the injected current flows through the connective tissue beneath the urothelium (in normal areas). However, most of the applied current flows through the surface fluid (at low frequency ranges) in normal bladder tissue. Finally, in the malignant area, at least 50% of the injected current flows beneath transformed urothelium across the whole frequency range modelled. This can lead us to improve our understanding how the current pass through different layers of the bladder tissues in different frequencies and different tissue states. Furthermore, device, system and methods for bioimpedance measurement of cervical tissue and methods for diagnosis and treatment of human cervix was improved in nowadays [24].

An approach is presented for studying the analysis of the mechanical behavior of the urinary bladder. A procedure for identifying the mechanical properties of the main constituents of the bladder tissue by an inverse method is detailed. The mechanical parameters are used for the numerical simulation of the mechanical behavior of the bladder during filling within the finite-element method [25].

Finally, it must be mentioned that we need more and more clinical trials with *in vivo* measurements to apply EIS technique in bladder cancer screening in the future.

References

1. Black, R. J., F. Bray, et al. (1997). "Cancer incidence and mortality in the European Union: cancer registry data and estimates of national incidence for 1990." Eur J Cancer 33(7): 1075-107.
2. Brown, B. H., J. A. Tidy, et al. (2000). "Relation between tissue structure and imposed electrical current flow in cervical neoplasia." Lancet 355(9207): 892-5.

3. Gonzales-Correa, C. A., B. H. Brown, et al. (1999). "Virtual Biopsies in Barrett's Oesophagus using an Impedance probe." Annals New York Academy of Sciences 873: 313-321.
4. Keshtkar, A., Z. Salehnia, et al. (2012). "Bladder cancer detection using electrical impedance technique (tabriz mark 1)". Patholog Res Int 470101
5. Liao, WC., FS Jaw (2011). " Noninvasive electrical impedance analysis to measure human urinary bladder volume". J Obstet Gynaecol Res. 2011 Aug;37(8):1071-5
6. Minsky, B. D. and F. J. Chlapowski (1978). "Morphometric analysis of the translocation of lumenal membrane between cytoplasm and cell surface of transitional epithelial cells during the expansion-contraction cycles of mammalian urinary bladder." J Cell Biol 77(3): 685-97.
7. Syrigos, K. N. and D. G. Skinner (1999). Bladder Cancer (Biology, Diagnosis and Management). Chapter 12, Oxford University Press.
8. Gonzales-Correa, C. A., B. H. Brown, et al. (2003). "Low frequency electrical bioimpedance for the detection of inflammation and dysplasia in Barrett's oesophagus." Physiol.Meas. 24: 291-296.
9. Keshtkar, A., R. H. Smallwood, et al. (2001). Virtual bladder biopsy by bioimpedance measurements. XI International Conference On Electrical Bio-Impedance, Oslo, Norway, Oslo University.
10. Keshtkar, A., A. Keshtkar, et al. (2006). "Electrical impedance spectroscopy and the diagnosis of bladder pathology." Physiological Measurement 27: 585-596.
11. Smallwood, R. H., A. Keshtkar, et al. (2002). "Electrical impedance spectroscopy (EIS) in the urinary bladder: the effect of inflammation and edema on identification of malignancy." IEEE Trans Med Imaging 21(6): 708-10.
12. Walker, D. C., R. H. Smallwood, et al. (2005). "Modelling the electrical properties of bladder tissue-- quantifying impedance changes due to inflammation and oedema." Physiol Meas 26(3): 251-68.
13. Wilson, A. J., P. Milnes, et al. (2001). "Mk3.5: a modular, multi-frequency successor to the Mk3a EIS/EIT system." Physiol Meas 22(1): 49-54
14. Keshtkar, A. (2007). "Design and construction of small sized pencil probe to measure bio-impedance." Med Eng Phys 29(9): 1043-8.
15. Gonzales-Correa, C. A. (2000). Endoscopic measurement of electrical impedance spectra and their dependence on tissue properties in barrett's oesophagus. Department of Medical Physics and Clinical Engineering. Sheffield, PhD thesis, Sheffield University.
16. Waterworth, A. R., P. Milnes, et al. (2000). "Cole equation modelling to measurements made using an impulse driven transfer impedance system." Physiol Meas 21(1): 137-44.
17. Keshtkar, A. and A. Keshtkar (2008). "The effect of applied pressure on the electrical impedance of the bladder tissue using small and large probes." J. Med. Eng. Technol., Vol. 32, No. 6, pp.505–511.
18. Keshtkar, A., A. Mesbahi, et al. (2008). "Surface fluids effects on the bladder tissue characterisation using electrical impedance spectroscopy." Medical Engineering and Physics 30: 693-699.
19. Keshtkar, A. and A. Keshtkar (2008). "Modelled Current Distribution Inside the Normal and Malignant Human Urothelium Using Finite Element Analysis." IEEE TRANSACTIONS ON BIOMEDICAL ENGINEERING 55(No.2): 733-738.
20. Keshtkar, A. (2004). Characterisation Of Human Bladder Urothelium Using Electrical Impedance Spectroscopy. Medical Physics and Clinical Engineering Dep. Sheffield, PhD thesis, Sheffield University.
21. Hanley, J. A. and B. J. McNeil (1982). "The meaning and use of the area under a receiver operating characteristic (ROC) curve." Radiology 143(1): 29-36.
22. Cole, K. S. and R. H. Cole (1941). "Dispersion and absorption on dielectrics. I.Alternating current characteristics." J Chem Phys 9: 341-51.
23. Ahad MA, SB. Rutkove (2009). "Finite element analysis of electrical impedance myography in the rat hind limb". Conf Proc IEEE Eng Med Biol Soc. 2009;2009:630-3
24. Gruewitch et al (2009), "Device, System And Methods For Bioimpedance Measurement of Cervical Tissue and Methods For Diagnosis And Treatment Of Human Cervix" ,Us Patent 0171234A1, 2009.
25. Shaofan Li., Dong Qian, et al. (2013)."Characterization of Mechanical Properties of Biological Tissue: Application to the FEM Analysis of the Urinary Bladder ". 21 MAR 2013, DOI: 10.1002/9781118402955.ch15